

An Air Route Planning Model of Unmanned Aerial Vehicles Under Constraints of Ground Safety

HAN Peng*, ZHAO Yifei

School of Air Traffic Management, Civil Aviation University of China, Tianjin 300300, P. R. China

(Received 1 March 2020; revised 18 May 2020; accepted 15 July 2020)

Abstract: With the rapid growth of the number and flight time of unmanned aerial vehicles (UAVs), safety accidents caused by UAVs flight risk is increasing gradually. Safe air route planning is an effective means to reduce the operational risk of UAVs at the strategic level. The optimal air route planning model based on ground risk assessment is presented by considering the safety cost of UAV air route. Through the rasterization of the ground surface under the air route, the safety factor of each grid is defined with the probability of fatality on the ground per flight hour as the quantitative index. The air route safety cost function is constructed based on the safety factor of each grid. Then, the total cost function considering both air route safety and flight distance is established. The expected function of the ant colony algorithm is rebuilt and used as the algorithm to plan the air routes. The effectiveness of the new air route planning model is verified through the logistical distribution scenario on urban airspace. The results indicate that the new air route planning model considering safety factor can greatly improve the overall safety of air route under small increase of the total flight time.

Key words: air transportation; unmanned aerial vehicle (UAV); air route planning; safety cost; ground risk assessment; improved ant colony algorithm

CLC number: TN925

Document code: A

Article ID: 1005-1120(2021)02-0298-08

0 Introduction

Unmanned aerial vehicles (UAVs) have been widely used in urban logistical and distribution in recent years. By June 2019, 337 000 industrial UAVs had been registered in China alone, with a total of more than one million flight hours^[1]. However, the safety accidents caused by UAV flight risks are increasing gradually. These accidents have had serious consequences for people and property on the ground. Before the explosive growth of UAVs, it is of great significance to study their flight safety.

According to the investigation and analysis of the previous UAV safety accidents, the characteristics of unmanned aircraft determine that the safety risk of UAV flight shifts from the impact on board to the ground. Joint authorities for rulemaking on unmanned systems (JARUS) issued the licensed oper-

ation risk assessment guidance material (SORA) for UAV operation scenarios and provided a general framework for UAV system operation risk assessment^[2]. SORA divided the potential damages of UAV operation into three categories, including the damages to the third party in the air, to the third party on the ground and to the critical infrastructure on the ground. The latter two were clearly defined as the main risks of UAV operations. In other words, the safety of ground people and property under the UAV air route became the key to the safety of UAV operations. Therefore, ground risk assessment should be considered in advance in the process of air route planning to make sure the mitigation of UAV flight risk.

In order to minimize the damage of UAV crashes to people on the ground at the level of strategic planning, safety risk assessment results should be

*Corresponding author, E-mail address: han_peng_2007@126.com.

How to cite this article: HAN Peng, ZHAO Yifei. An air route planning model of unmanned aerial vehicles under constraints of ground safety[J]. Transactions of Nanjing University of Aeronautics and Astronautics, 2021, 38(2):298-305.

<http://dx.doi.org/10.16356/j.1005-1120.2021.02.010>

added to air route planning in advance. Scholars and scientific institutions have conducted lots of studies in ground risk assessment affected by UAV operations. Ground risk was described as the uncertainty of UAV system failure under specific system configuration, operating environment conditions and missions^[3-6]. Ground impact area of UAV crashes^[7-10] was described as the probability distribution of the impact area after the crash. Ground object exposure distribution^[7,11-12] was described as the probability of the presence of damaged objects (people and property) at a specific location and time. The exposed object distribution model can be divided into unified model and comprehensive model. Injury model caused by UAV crashes^[13-14] was described as the severity of the drone's damage to humans or property at the specific time and place.

From the forward flow, these models have been widely used in the evaluation of UAV flight safety. However, from the perspective of reverse flow, ground risk assessment is rarely used in air route planning. A new air route planning method based on ground risk assessment and its calculation method are proposed in this paper which focuses on an air route planning method based on ground risk assessment and its algorithm.

1 Air Route Planning Model

1.1 Analysis of air route planning

At present, studies on air route planning methods^[15-18] fall into two categories. One is based on intelligent algorithms, such as intelligent bionics and particle swarm optimization, and the other is based on graphical algorithms, such as Voronoi diagrams and Laguerre diagrams. Through the analysis of the existing literature, we found that most studies on path planning focused on the optimization of the distance cost and smoothness of the air route. However, due to the important role of air route in safety, ground risk assessment^[19-21] should be considered in air route planning.

In order to ensure the safe and convenient flight of UAVs, two objectives should be considered in the process of air route planning: Safety cost and

distance cost. As shown in Fig.1, the safety cost in route planning focuses on the impact of UAV flight on the ground casualties below the route, and the optimization function should be built based on the safety index of risk assessment. The distance cost mainly considers the obstacle avoidance, flight distance and non-linear coefficient.

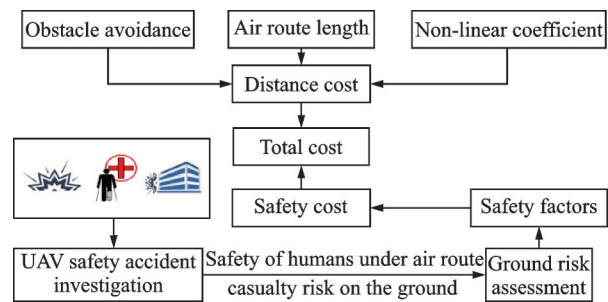


Fig.1 Cost model of UAV air route planning

1.2 Ground risk assessment

As shown in Fig.2, the UAV system and ground characteristics are two major considerations in ground risk assessment. Reliability and failure probability are related to the probability of UAV crashes. The impact area of a crash is calculated according to the dynamics and kinematics characteristics. From the perspective of the ground people, the protective ability of ground cover and the population density have a great influence on the accident severity.

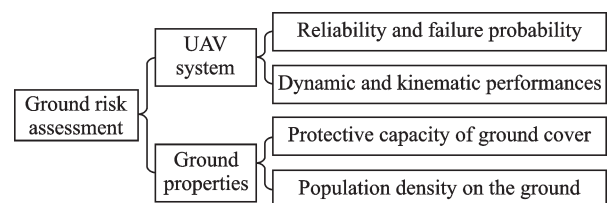


Fig.2 Influence factors of ground risk assessment

1.2.1 Grid division of the ground surface

In order to evaluate the safety costs on the ground, the ground surface below the air route should be rasterized first. In order to ensure the integrity of safety accident analysis within the grid, it is assumed that when the UAV falls in the center of the grid, the impact area of the accident falls completely within the grid. Therefore, it is necessary to analyze the area affected by an UAV crash in order to select the appropriate grid edge length. Fig.3 shows the ar-

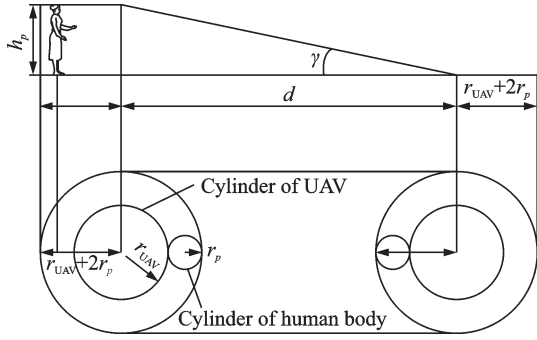


Fig.3 Area affected by UAV crashes

ea affected by an UAV crash accident, which is defined as the maximum range of human body cylinder invaded by the UAV cylinder. When only the vertical movement of the UAV is considered, the area affected by the accident can be expressed as

$$A_{gv} = \pi(r_{UAV} + 2r_p)^2 \quad (1)$$

where r_{UAV} represents the equivalent wingspan radius of the UAV and r_p the radius of human body.

Further, the horizontal displacement still needs to be considered after the collision between the UAV and the human body. The horizontal displacement could be calculated by

$$d = \frac{h_p}{\tan \gamma} \quad (2)$$

where h_p represents the height of human body and the parameter γ the contact angle of the collision between the UAV and the human body. The area affected by the accident can be expressed as

$$A_g = 2\pi(r_{UAV} + 2r_p)^2 + (r_{UAV} + 2r_p)d \quad (3)$$

According to the above analysis, the grid edge length can be calculated by

$$l = 2(r_{UAV} + 2r_p) + d \quad (4)$$

1.2.2 Grid safety factor

In order to quantify the flight safety attributes of UAVs in the barrier-free grid, the risk of casualties caused by UAV collision accidents to ground people is analyzed. The safety factor of each grid is defined as the number of casualties caused by UAV collision accidents per flight hour. The safety factor could be expressed in terms of the probability of UAV collision accidents, the probability of casualties after accidents and the total population affected by accidents, namely

$$s = P_{gs} \times P_{fgs} \times N_{exp} \quad (5)$$

where the parameter s represents the safety factor of

the grid defined by the number of ground casualties per flight hour. P_{gs} and N_{exp} represent the probability of UAV collision accidents and the total population on the ground affected by accidents, respectively.

1.2.3 Probability of fatality

The probability of fatality^[14] affected by UAV collision accidents in each grid is related to a few factors, including the UAV characteristics and grid properties. The UAV characteristic factors are related to the operating altitude and velocity. The grid properties are in connection with the protection capability that can be provided by the shelter in the grid and the population density. The probability of fatality is shown as follows

$$P_{fgs}(j) = \frac{1 - n}{1 - 2n + \sqrt{\frac{\alpha}{\beta} \left[\frac{\beta}{E_{imp}} \right]^{P_s(j)}}} \quad (6)$$

where the parameter α is the impact energy required for a fatality probability of 50% when $P_s = 6$, which can be valued as 100 kJ normally. The parameter β represents the impact energy threshold when P_s goes to 0, which can be considered to be a constant with 34 J based on fatality limit. The parameter E_{imp} is the kinetic energy when the ground impact accident occurs. The speed used when calculating E_{imp} is higher than the vertical falling speed and 1.4 times of the maximum design speed^[22]. P_s represents the total protection factor of the grid which related to the category and area of the shelters onto the surface. The protection factor of different shelters is listed in Table 1. The total protection factor can be calculated according to the percentage of each shelter area as follows

$$P_s(j) = \sum_{h=1}^H P_s^h \frac{M_h}{M_j} \quad (7)$$

where the parameter h represents the category of shelters and P_s^h the protection factor of shelter h . M_h and M_j represent the area of shelter h and total area of the grid, respectively.

Table 1 Ground shelter classification and protection factor

Shelter type	Concrete buildings	Tall trees	Sparse trees	Surface
Protection factor	10	7	4	0

1.3 Air route cost

The purpose of the route planning method proposed in this paper is to find a safe and short air route from the origin to destination under the premise of avoiding obstacles. Therefore, the total air route cost function under the dual constraints of safety cost and distance cost is constructed as follows

$$d'_j = \lambda \times d_{jd} + \mu \times s_j \quad (8)$$

2 Algorithm of Air Route Planning

The ant colony algorithm is selected as the method of solving the route planning problem. In order to satisfy the cost function as mentioned above, it is necessary to improve the expected function of ant colony algorithm first. The total cost function of air route in section 1.3 is taken as the expected function of air route planning.

2.1 Calculation flow

The calculation flow of the improved ant colony algorithm is shown in Fig.4. The ant colony

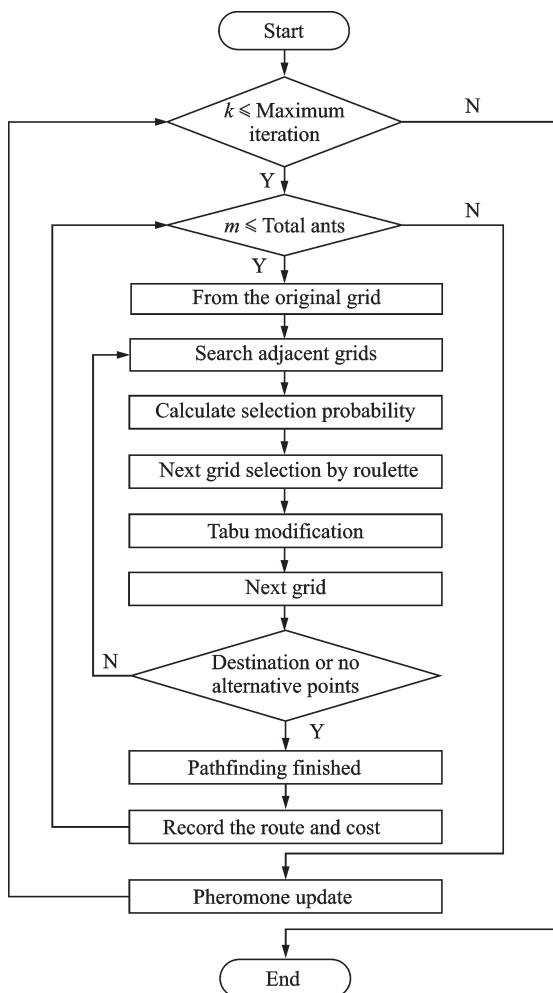


Fig.4 Flow chart of improved ant colony algorithm

starts from the original grid and searches the barrier-free adjacent grids. The selection probability of each adjacent grid is based on the expected cost function. The determination of the next grid is according to the results of the roulette method. The whole process is over until the ants get to the destination or trap in a local optimal solution. After the iteration of appropriate generations, the expected air route optimized by both safety and distance costs is finally obtained.

2.2 Algorithm improvement

The traditional ant colony algorithm has limitations for wide-range route search. The problems encountered in the study mainly include three aspects^[15]. First, the search space is too large, which leads to low efficiency and slow convergence speed. Second, search step size is small which is not suitable for long distance search. Third, there is no direction to inspire the search strategies which may produce path circuitous redundancy. To solve these problems, search space range and variable search radius are adopted to improve the traditional ant colony algorithm. Specifically, the problem of search efficiency can be solved by reasonably controlling the size of search space. The line between the starting and stopping points is used as the buffer of variable distance to form the search space (Fig.5). The buffer distance increases gradually from the initial value until there is an optimal route solution in the search space. At the same time, in order to improve the efficiency of path search, variable length search is adopted in the search process, that is, the search step size is determined according to the safety factors in the local search space. For example, when the safe-

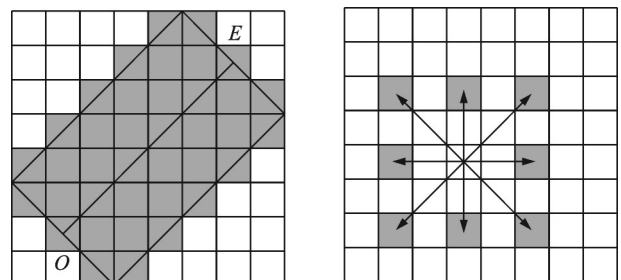


Fig.5 Search space range and variable search radius of improved ant colony algorithm

ty factors in the search space are less than 10^{-7} , the step size adopts two grid units, as shown in Fig.5.

2.3 Probability calculation of optional adjacency grid and pheromone update

The selection probability of each adjacent grid for next step is calculated by

$$P_{ij}^k(t) = \begin{cases} \frac{[\tau_{ij}(t)]^\xi [\eta_{ij}(t)]^\psi}{\sum_{s \in \text{allowed}_k} [\tau_{is}(t)]^\xi [\eta_{is}(t)]^\psi} & j \in \text{allowed}_k \\ 0 & j \notin \text{allowed}_k \end{cases} \quad (9)$$

where P_{ij}^k is the probability of the k th ant moving from point i to point j , the parameter allowed_k the nodelist that the ant is allowed to access in the next step, τ_{ij} the concentration of pheromone from point i to point j , η_{ij} the expectation from point i to point j which is calculated by the total cost function established in Eq.(8), ξ the pheromone heuristic coefficient which represents the importance of pheromone, and ψ the expectation heuristic coefficient which represents the importance of expectation. Pheromone concentration is updated after the preset iterations, and the update rule is shown in

$$\tau_{ij}(t) = (1 - \rho)\tau_{ij} + \sum_{k=1}^m \Delta\tau_{ij}^k \quad (10)$$

$$\Delta\tau_{ij}^k = \begin{cases} \frac{Q}{C_k} & \text{Component } (i,j) \text{ is used} \\ 0 & \text{Otherwise} \end{cases} \quad (11)$$

where $\Delta\tau_{ij}^k$ is the pheromone concentration increase of the k th ant from point i to point j , ρ the pheromone volatility coefficient which values from 0 to 1, Q the pheromone enhancement coefficient, and C_k the crawling distance from the origin to the destination of the k th ant.

In order to avoid falling into the local optimum in the path search process, in the transfer probability calculation of the track point transfer process, the connection between the current node and the termination node is introduced into the heuristic function according to the evaluation function in the A* algorithm. It can solve the local optimum problem and improve the efficiency of the algorithm. The heuristic function is as follows

$$\eta_{ij}(t) = \begin{cases} (1 - C \times \overline{d'_{Oj}}) \times \overline{d'_{Oj}} + C \times \overline{d'_{Oj}} \times \overline{d'_{jE}} & \rho < d'_{Oj} < d'_{jE} \\ \frac{1}{d'_{ij}} & \text{Otherwise} \end{cases}$$

$$\overline{d'_{Oj}} = \frac{d'_{Oj}}{\sum_{j \in \text{allowed}_k} (d'_{Oj} + d'_{jE})}$$

$$\overline{d'_{jE}} = \frac{d'_{jE}}{\sum_{j \in \text{allowed}_k} (d'_{Oj} + d'_{jE})} \quad (12)$$

where d' represents the cost and $\overline{d'}$ the cost after normalization. The subscript in the formula represents the node code, O the original point, and E the ending point. i and j represent the node number in the path. $C \times \overline{d'_{Oj}}$ represents the weight of the cost between next node and the end point; ρ represents the path cost threshold that starts to introduce direction information, in order to prevent ants from being affected by direction information and falling into local optimality in the process of moving. C and ρ are constant which determined in practical application.

3 Application to Logistical Distribution Scenario in Urban Air-space

3.1 Description of task scenario

UAV logistical distribution has the advantage of reducing human contact. It has strong practicability in urban emergency supplies and medicine distribution during the period of COVID-19. UAV logistical distribution in Jiangnan district of Wuhan is selected as a typical case. In this case, the UAVs are used to carry out the express delivery and catering services on this area.

3.2 Parameters of UAVs

The Maxi Joker 2 is selected as the delivery drone, and the main design parameters are shown in Table 2. The small design mass and moderate speed are suitable for small-batch and high-frequency flight activities in urban airspace. It is assumed that the probability of safety accidents caused by UAV system failure is 10^{-5} per flight hour. The influence of

environment on the reliability of UAV is not considered in the model.

Table 2 Parameters of Maxi Joker 2

Type	Mass/kg	Design speed/ ($\text{m}\cdot\text{s}^{-1}$)	Rotor length/m
Maxi Joker 2	8	20	1.8

3.3 Ground surface rasterization

The distribution of the surface coverage on the ground is mapped as shown in Fig.6, where different grayscale represents different land use classification. Hankou railway station is selected as cargo storage place and three hospitals are selected as the shipping address. Two different kinds of air route planning methods are used to show the roles of safety factors. The first method takes safety factors and distance into considerations, as shown in Eq.(9), while the second method only takes distance as the constraint. The flight distance, flight time, average route safety factor and casualty population of the different planned air routes, considering the safety cost or not, are compared.

According to the parameters in Table 2 and the grid size calculation method in Section 2.2, the grid

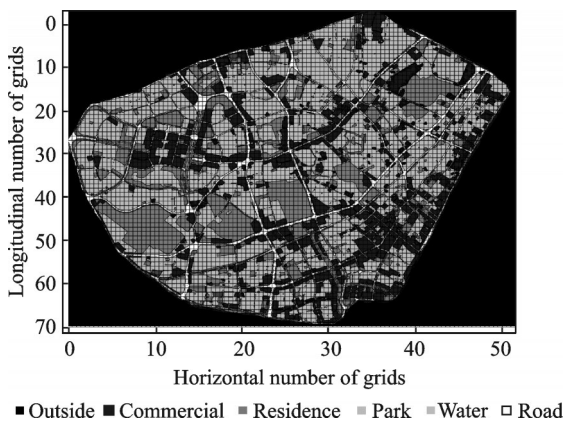


Fig.6 Distribution of surface coverage over the ground in flight area

size is set as $100\text{ m}\times 100\text{ m}$, and a 73×103 grid array is constructed to cover the area completely. Based on the distribution of surface coverage and the protection factor provided by different kinds of shelters on the ground in Table 1, the protection factor of ground grids in the flight area is calculated by Eq.(8).

The ground population density corresponding to the flight area is an important variable for evaluating the risk severity of UAV collision accidents. The population data on this area is collected by mobile carrier data. The population distribution data collected at 15:00 is used, and the population distribution density map is shown in Fig.7.

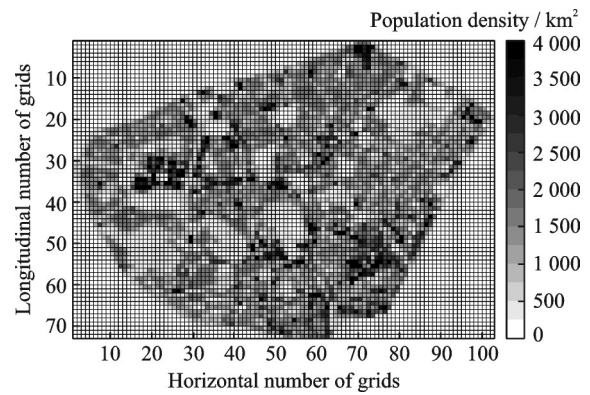


Fig.7 Grayscale map of population distribution density map in each ground grid

The safety factor of the grids is calculated by the protection factor and population density.

3.4 Comparisons of planned air routes

The calculation results of the main indicators for the planned air routes from origin EP to each destination SP are shown in Table 3. Taking the planned air route from SP3 to EP as an example, the flight distance of the planned route with safety

Table 3 Comparison of main technical indexes of each planned air route

Planned air routes	From SP1 to EP			From SP2 to EP			From SP3 to EP		
	With safety cost?		Change rate/%	With safety cost?		Change rate/%	With safety cost?		Change rate/%
	No	Yes		No	Yes		No	Yes	
Flight distance/m	4 066	4 314	6.1	4 270	4 363	2.2	6 197	6 777	9.4
Flight time /s	203	216	6.1	213	218	2.2	310	339	4.3
Average safety factor/ 10^{-5}	4.9	2.7	-44.9	4.5	2.2	-51.1	5.7	2.3	-59.7
Total casualty population/ 10^{-7}	1.65	0.95	-42.4	1.6	0.8	-50	2.9	1.3	-55.2

constraint is 6 777 m, which is 580 m longer than that of the planned air route without safety constraint, with an increase rate of about 9.4%. However, the average safety factor of the route through the grid is decreased from 5.7×10^{-5} to 2.3×10^{-5} , with a safety improvement of 59.7%. The total casualty population on the route had been reduced from 2.9×10^{-7} to 1.3×10^{-7} .

Therefore, the overall route safety has been greatly improved on the premise of a small increase in total length and flight time when taking safety factors into consideration. As shown in Fig.8, the air route changes locally when the safety constraints are considered. The flight distance and flight time increase slightly compared with the planned air route without safety constraints. But the average safety factors of planned air route decrease to a great extent. At the same time, the casualty population in the whole air route decrease as well.

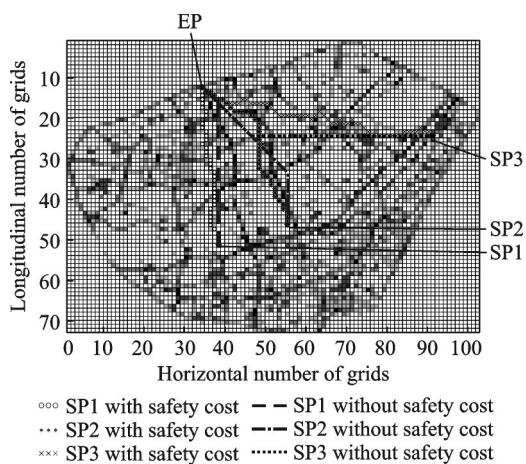


Fig.8 Comparison of planned air routes with or without safety

4 Conclusions

A new kind of air route planning model considering the dual optimization conditions of safety and distance is established. The safety constraints in the model are based on the ground risk assessment under the air route. The effectiveness of the new air route planning model is verified through the logistical distribution scenario in urban airspace. By comparing the main technical indexes of planned air routes with or without safety constraints, the results show that

the safety of the planned air routes is significantly improved after considering the safety factors, while the total length and flight time of the planned air routes are slightly increased. The new air route planning model with safety factors improves the overall safety of the planned air route greatly when the distance cost increases to an acceptable level.

References

- [1] Civil Aviation Administration of China. Annual report of China civil aviation unmanned aerial vehicle operation management 2018[R]. Beijing: Civil Aviation Administration of China, 2019.
- [2] Joint Authorities for Rulemaking of Unmanned Systems (JARUS). JARUS guidelines on specific operations risk assessment (SORA); JARUS WG-6 Leader [R]. Swiss: [s.n.], 2017.
- [3] AALMOES R, CHEUNG Y S, SUNIL E, et al. A conceptual third-party risk model for personal and unmanned aerial vehicles[C]//Proceedings of 2015 International Conference on Unmanned Aircraft Systems. Denver, CO, USA: IEEE, 2015.
- [4] BARR L C, NEWMAN R, ANCEL E, et al. Preliminary risk assessment for small unmanned aircraft systems[C]//Proceedings of the 17th AIAA Aviation Technology, Integration, and Operations Conference. Colorado: AIAA, 2017.
- [5] LUM C, WAGGONER B. A risk-based paradigm and model for unmanned aerial systems in the national airspace[M]. Missouri: Aerospace, 2011.
- [6] WOLF S E. Modeling small unmanned aerial system mishaps using logistic regression and artificial neural networks[R]. Dayton: Air Force Institute of Technology, 2012.
- [7] ANCEL E, CAPRISTAN F M, FOSTER J V, et al. Real-time risk assessment framework for unmanned aircraft system (UAS) traffic management (UTM)[C]//Proceedings of the 17th AIAA Aviation Technology, Integration, and Operations Conference. Denver: AIAA, 2017.
- [8] ANDERS L, SCHIOLER H. Ground impact probability distribution for small unmanned aircraft in ballistic descent[C]//Proceedings of International Conference on Unmanned Aircraft Systems. Athens: Institute of Electrical and Electronics Engineers, 2020: 1-16.
- [9] HAARTSEN Y, AALMOES R, CHEUNG Y S. Simulation of unmanned aerial vehicles in the determination of accident locations[C]//Proceedings of 2016 International Conference on Unmanned Aircraft Systems. Arlington: IEEE, 2016: 993-1002.
- [10] STEVENSON J D, YOUNG S, ROLLAND L. Estimated levels of safety for small unmanned aerial vehi-

- cles and risk mitigation strategies[J]. *Journal of Unmanned Vehicle Systems*, 2015, 3(4): 205-221.
- [11] ANDREW D, KNOTT M, BURKE D. Population density modeling tool[R]. Maryland: Department of the Navy, Naval Air Warfare Center Aircraft Division, 2012.
- [12] GUGLIERI G, QUAGLIOTTI F, RISTORTO G. Operational issues and assessment of risk for light UAVs[J]. *Journal of Unmanned Vehicle Systems*, 2014, 2(4): 119-129.
- [13] BALL J A, KNOTT M, BURKE D. Crash lethality model[R]. Maryland: Naval Air Warfare Centre Aircraft Division, 2012.
- [14] DALAMAGKIDIS K, VALAVANIS K P, PIEGL L A. On integrating unmanned aircraft systems into the national airspace system: Issues, challenges, operational restrictions, certification, and recommendations[M]. London: Springer Science & Business Media, 2011.
- [15] XU Chenchen, LIAO Xiaohan, YUE Huanyin, et al. Construction of a UAV low-altitude public air route based on an improved ant colony algorithm[J]. *Journal of Geo-information Science*, 2019, 21(4): 570-579. (in Chinese)
- [16] ZHANG Xuejun, LIU Yang, ZHANG Yu, et al. Safety assessment and risk estimation for unmanned aerial vehicles operating in national airspace system[J]. *Journal of Advanced Transportation*, 2018(2): 1-11.
- [17] QIN W, ZHANG J, SONG D. An improved ant colony algorithm for dynamic hybrid flow shop scheduling with uncertain processing time[J]. *Journal of Intelligent Manufacturing*, 2018, 29(4): 891-904.
- [18] WANG L, XIA X H, CAO J H, et al. Improved ant colony-genetic algorithm for information transmission path optimization in remanufacturing service system[J]. *Chinese Journal of Mechanical Engineering*, 2018, 31(6): 106-117.
- [19] GONCALVES P, SOBRAL J, FERREIRA L A. Unmanned aerial vehicle safety assessment modelling through petri nets[J]. *Reliability Engineering and System Safety*, 2017(167): 383-393.
- [20] MELNYK R, SCHRAGE D, VOLOVOI V, et al. A third-party casualty risk model for unmanned aircraft system operations[J]. *Reliability Engineering & System Safety*, 2014(124): 105-116.
- [21] DONATO P F A, ATKINS E M. Evaluating risk to people and property for aircraft emergency landing planning[J]. *Journal of Aerospace Information Systems*, 2017, 14(5): 259-278.
- [22] KOH C H, LOW K H, LIL, et al. Weight threshold estimation of falling UAVs (Unmanned aerial vehicles) based on impact energy[J]. *Transportation Research Part C: Emerging Technologies*, 2018(93): 228-255.

Acknowledgement This work is supported by the Scientific Research Project of Tianjin Education Commission (No.2019KJ128).

Author Dr. HAN Peng received his Ph.D. degree in vehicle operation engineering from State Key Laboratory of Traction Power, Southwest Jiaotong University. He participated in a joint workshop on Ph.D. education in University of Illinois at Urbana Champaign in 2013. Currently he is a lecturer at school of Air Traffic Management, Civil Aviation University of China. His main research interests are in UAV operation and air traffic control.

Author contributions Dr. HAN Peng designed the study, compiled the models, conducted the analysis, and wrote the manuscript. Prof. ZHAO Yifei contributed to the discussion, interpreted the results and background of the study. All authors commented on the manuscript draft and approved the submission.

Competing interests The authors declare no competing interests.

(Production Editor: XU Chengting)

基于地面安全约束的无人机航路规划研究

韩 鹏, 赵焱飞

(中国民航大学空中交通管理学院, 天津 300300, 中国)

摘要:随着无人机数量和飞行时间的快速增长,由无人机飞行风险引起的安全事故也逐渐增多。安全航路规划是在战略层面降低无人机运行风险的有效手段。考虑无人机航路的安全代价,基于地面风险评估提出了一种无人机安全航路规划模型。将航路下方区域栅格化处理,以每飞行小时地面人员伤亡率为量化指标,定义各栅格安全系数,并根据栅格安全系数构造航路安全代价函数。建立了兼顾航路安全性和飞行距离的总代价函数,并通过改进蚁群算法进行航路规划。模型的有效性通过城市空域物流无人机航路规划进行验证。结果表明,考虑地面安全约束的航路规划模型在无人机总飞行时间增加不大的情况下,能显著提高航路的整体安全性。

关键词:航空运输;无人机;航路规划;安全代价;地面风险评估;改进蚁群算法